# Experimental investigation on a combined solar and ground source heat pump system for a single-family house: Energy flow analysis and performance assessment

Changxing Zhang[a,b,*], Elsabet Nielsen[b], Jianhua Fan[b,*], Simon Furbo[b], Qingqing Li[c]

[a]*Shandong Key Laboratory of Civil Engineering Disaster Prevention and Mitigation, Shandong University of Science and Technology, Qingdao 266590, PR China*

[b]*Department of Civil Engineering, Technical University of Denmark, Lyngby 2800, Denmark*

[c]*School of Civil Engineering and Architecture, Qingdao Agricultural University, Qingdao, 266000, PR China*

http://doi.org/10.1016/j.enbuild.2021.110958

**Abstract:** This paper presents experimental investigations on a combined solar and ground source heat pump (SGHP) system for a single-family house. The SGHP system was installed at the Lyngby campus of Technical University of Denmark with horizontal ground heat exchanger (HGHE). Detailed experiments were carried out on the system in 2019 under real weather conditions and the heating demand for domestic hot water (DHW) and space heating (SH). The focuses of the investigation are energy flow analysis and performance assessment on the SGHP system. The results showed that the yearly system seasonal performance factor of the SGHP system ($SPF_{SHP}$) was 2.8, and the maximum monthly $SPF_{SHP}$ was up to 5.7 in April with the highest solar radiation. Directly utilized solar energy for the combi-storage was 500 kWh lower than the annual solar heat for charging the ground, and it accounted for 38% of annual heat input of the combi-storage, the rest of the heat was supplied by the heat pump system that consumed 84% of total electricity energy. Different from the large fluctuations of monthly solar fraction due to solar radiation, the monthly renewable heat fraction was within the range from 57% to 83%, and the yearly value was 65%.

**Keywords:** Combined solar and ground source heat pump system; Experiment; Seasonal performance factor; Renewable heat fraction; Solar fraction

*Corresponding authors.
*E-mail addresses:* zcx952@163.com (C. Zhang), jif@byg.dtu.dk (J. Fan)

# 1. Introduction

With fast development of human society, energy consumption is increasing rapidly, and it has more than doubled in the past 30 years. Energy consumption of residential buildings accounts for approximately 27% of the total energy consumption worldwide. For the energy consumption of residential buildings in Europe, 64.1% is spent on space heating (SH), 14.8% on water heating, 14.4% on electrical appliances and approximately 5.6% on cooking. Renewable energies contributes to 18% of EU's final energy consumption in households, which is mostly used for SH and domestic hot water (DHW) in 2017[1]. For residential buildings, solar heating systems and heat pumps are two promising renewable energy technologies for SH and DHW. According to a survey on heat sources for residential buildings [2], multisource systems based on combining solar energy and other heat sources, e. g. heat pumps or gas boilers account for about 21%, half of them are combined solar and ground source heat pump (SGHP) systems. Based on how solar heating and heat pump interact, parallel, serial, and regenerative arrangements could be applied, but they do not exclude each other within one system[2]. For the regenerative mode shown in Fig.1, solar collectors are usually used to improve the quality of ground heat source for long timescales when there are high solar radiation and low heating demand. Meanwhile, solar collector stagnation in summer can be prevented efficiently. Compared with the other two arrangements/modes, there is a lack of detailed investigations in literature on the energetic performance of the regenerative system. It is necessary for the regenerative system to maximize the interactive energy-saving potential of solar and ground heat energy according to load demands and the weather conditions in the whole year.

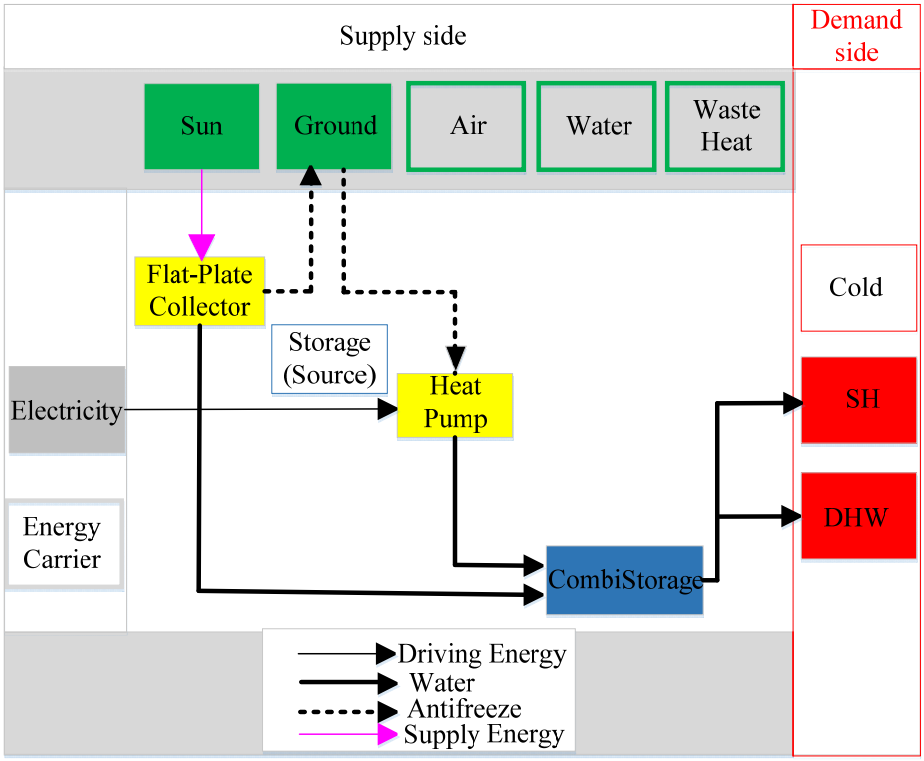


**Fig.1** The visualization of SGHP system with the regenerative arrangement

## *1.1* ***Simulation studies on SGHP system in residential building***

Many simulation studies on the regenerative arrangement of SGHP system for SH and DHW in residential building were carried out to investigate whether the use of solar energy to recharge the ground can improve the efficiency of SGHP system for a long-term period. By simulating the seasonal performance factor (*SPF)* for the heat pump in a SGHP system of a single-family dwelling, Kjellsson et al.[4] found that the best savings of electricity occurred when solar heat was used for DHW during summer and recharging borehole heat exchangers (BHE) during winter, and natural recharge was enough to cover the charging solar energy outtake during the heating season for a single BHE [4]. Razavi et al. focused on five different scenarios of SGHP system applied in a residential house located in Zahedan, Iran[5]. The energy consumption of the best SGHP system scheme was decreased with 8.7% compared to that of a ground source heat pump system, in which solar energy is prioritized to provide DHW and SH is only provided by heat pump system. Considering the technical and economical potential of solar PVT integration into ground source heat pump systems in multi-family houses in the Stockholm region, Sommerfeldt et al. [6] showed

that PVT was an economically viable alternative to drilling cost in undersized BHEs, and BHE length could be effectively reduced by 65% using Photovoltaic-Thermal (PVT) collectors in the case where auxiliary boiler consumption was high. For SGHP systems for residential buildings, it has been confirmed that passive natural and active ground regeneration were helpful to keep more stable long-term performance in three Baltic countries [7], but active ground regeneration could result in lower SPF due to specifically high electrical energy consumption used for ground regeneration. Miglani S et al. [8] presented a thermal model of ground source heat pumps coupled with BHE and solar regeneration for a single-family residential building in Zurich, Switzerland. The optimal BHE length of 160 m was obtained corresponding to the solar collector area of 50 $m^2$. The Simulated results of optimal scenarios indicated that continuous heat extraction by heat pump caused the ground temperature reduce to almost 5 °C in winter from the initial temperature of 11.5 °C, and solar regeneration increased the temperature back above initial temperature in summer. As mentioned above, the simulated results were influenced by many criteria including the operation conditions, the heating load, the component size, the typical geological and meteorological parameters, etc., and it is hard to say that the predicted energy saving can be obtained properly in practical project. Experimental studies are therefore needed to examine the actual performance of SGHP system and to validate the simulation models under local conditions.

In order to investigate the practical performance of SGHP systems for DHW and SH in residential buildings, numerous experiments have been conducted all over the world. Trillant-Berdal et al. [9] carried out an experimental study on a SGHP system for SH and DHW in a 180$m^2$ private residence. Energy injected into the ground represented 34% of the heat extracted, and the *COP* of the heat pump in heating mode had an average value of 3.75 in a period of 11 months. Wang et al.[10] made an experimental study of a SGHP system with a solar seasonal thermal stirage installed in a 120 $m^2$ detached house in Harbin. With the solar collector area of 50 $m^2$, the results showed that the solar heat directly supplied by the solar collectors accounted for 49.7% of the total experimental heating demand of 144.45 GJ, and the heat extracted from the soil by the heat pump

accounted for 75.5% of the heat stored by solar seasonal thermal storage after a year of operation. In order to estimate the efficiency of a solar energy storage under ground using a U-tube GHE, Verma and Murugesan [11] charged solar heat to the GHE from 9 am to 5 pm and discharged stored heat for SH in the night time from 7 pm to 3 am by adjusting the operation mode of GSHP system. It was concluded that charging of the ground resulted in 23% increase of the $Cop_s$ for SH. Carlos et al. [12] carried out an experimental investigation on a SGHP system providing DHW and SH for a two-storey late 19th-century house in Leicester, UK. They designed "Earth Energy Bank" to store heat seasonally where 16 short BHEs of 1.5 m depth in series were insulated with polyisocyanurate on the top and sides. The results showed that solar heat injected in the ground was useful not only to recover the soil from the thermal imbalance but also to store heat. Huang J et al.[13] monitored the large scale SGHP system for heating and cooling of a village with 450 inhabitants in Beijing. They found system COP increased by 9.4% from 2.42 to 2.65 and the annual overall operating cost decreased by adding DHW load that was 13.8% of the total heating load of the whole village. To maintain the energy quality with high temperature and reduce the energy loss of seasonal heat-storage in SGHP system, Sun T et al. [14] designed a novel SGHP system with the heat-cascading of BHEs and carried on a field-test in a community in Shandong province, China. It is proved that the solar heat cascade storage and utilization contributed the improvement of the system performance.

An experiment with a SGHP system in a heating-dominated climate zone in Poland was presented by Rynkowski P [15]. The results showed the active ground regeneration in summer could cause soil to be in a state of thermal equilibrium and improve efficiency of SGHP system in winter, and the average efficiency ratio of the heat transferred from solar radiation to the soil was 42.3% in the active ground regeneration.

According to the literature survey, most of numerical and experimental studies on SGHP system have used BHEs as the charging/discharging heat component of ground source. In fact, BHE at shallow depth and horizontal slinky-type GHE can efficiently improve the system performance, and

HGHE can extract more solar heat with more surface area under the free solar radiation in summer, which also makes it more suitable for single-family houses from the point of capital cost. Solar collectors and HGHE are combined to supply heat to combi-storage for DHW and SH by coupling heat pump with HGHE, and the regenerative mode between them is automatically started up based on the fluid temperature difference between solar collectors and HGHE, which is a parallel-regenerative SGHP system with energy-saving potential in single-family houses. How does solar energy contribute the heating demanding and charging the ground, and could the ground be automatically switched between charging by solar energy and discharging for the heating demand by heat pump under various weather conditions? Detailed experimental investigations are needed to understand the operation of the systems and improve thermal performance of the parallel-regenerative SGHP systems.

### *1.2* ***Scope***

This paper proposes a HGHE-coupled SGHP system with combi-storage for a single-family house, and experimental investigations on its thermal performance were carried out in 2019. The analysis gives an understanding of the dynamic behaviour of the SGHP system and the different operation characteristics under various weather conditions. Firstly, monthly energy flows are measured and summarized for the different weather conditions, and energy balance of the SGHP system under continuous heating load is analysed using measured electricity consumptions of different components. Secondly, the energy flows of the different components are evaluated to give an understanding of the synergy between direct solar utilization, heat pump heating and regenerative HGHE. At last, solar fraction is used to analyze the share of the direct solar energy, and the full potential of SGHP system to use solar energy and ground heat energy is assessed by the monthly renewable heat fraction.

## 2. Experimental system description

### *2.1 Components of the SGHP system with HGHE*

A SGHP system with HGHE was installed and measured at the test area of the Technical

University of Denmark. The latitude of the test area is 56°N. The SGHP system consists of a tank-in-tank combi-storage, evacuated tubular collectors, a water-to-water heat pump and a HGHE. The system is subject to real weather conditions and is equipped with automated draw offs for DHW and SH to replicate realistic demand in a single-family house. An illustration of the SGHP system is shown in Fig.2 with measurement and controller sensors location indicated. Table1 lists the main components of the SGHP system.

As a heat storage equipment, a combi-storage for DHW and SH in SGHP systems for single-family house is highly welcome in comparison to most of systems with two separate tanks for DHW and SH. Moreover, a combi-storage has a better surface to volume ratio compared with two storage tanks and it has only one device where the ground and solar heat have to be conveyed, which simplifies hydraulics and control of the system [16]. Due to thermal stratification of water produced by temperature-dependent density in the combi-storage [17], high temperature water at the top of the store is delivered as DHW, and lower temperature water in the middle region of the store is available for SH. As seen in Fig 2, the combi-storage is a tank-in-tank heat storage with DHW in the inner tank and still water for SH in the outer tank. In the still water tank, a stratification polypropylene pipe with lockable openings acting as “non-return” valves [18] is used to ensure a good thermal stratification during charge of the tank with solar heat. Four specially fabricated pipes in the combi-storage are installed for charging of the tank with heat from the heat pump. With the arrangement of the pipes, water in the upper part of the inner tank has a relatively higher temperature and the top water is therefore used to provide DHW, while water in the middle of the store has a relatively lower temperature, and therefore used for SH. The return water from the SH loop is led into the tank via a direct inlet located under a half ball baffle plate in order to avoid mixing in the combi-storage. Except for the outlet to the SH loop which is located in the upper part of the store, all other inlet and outlet pipes enter the store through the bottom wall. The combi-storage was insulated with mineral wool whose thermal conductivity is 0.45 W/(m·K). and the

whole insulated tank was covered by aluminium foil. The insulation thickness on the top of the tank is 200 mm, and it is 50 mm around the tank. The tank bottom is not insulated.

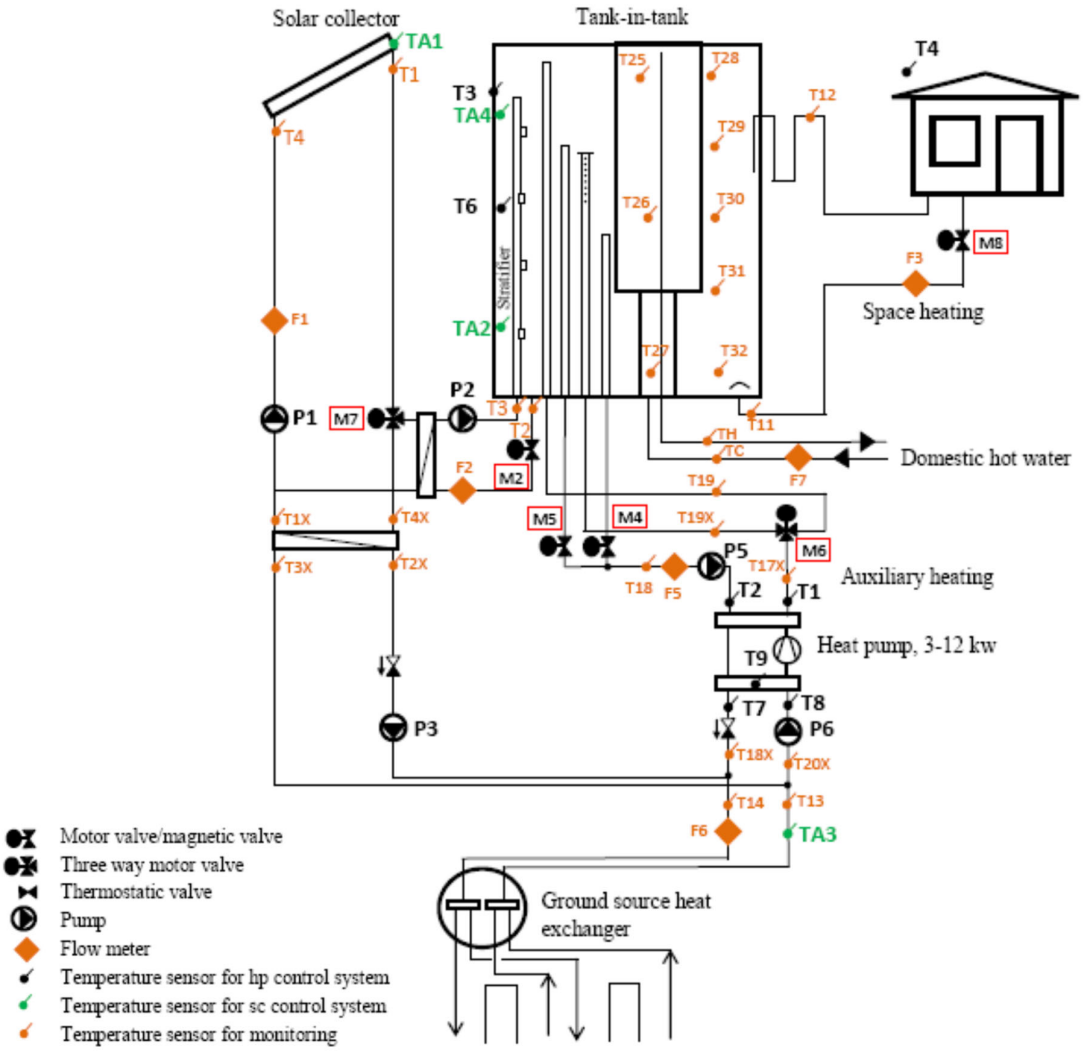


a) The SGHP system

b) Solar collectors

c) Combi-storage and heat pump

**Fig.2** An illustration of the SGHP system with measurement and controller sensors locations

**Table 1** The main components of the presented SGHP system

| Component | Description |
|---|---|
| Solar collector | 9.6 $m^2$, Evacuated tubular collector, Kingspan |
| The combi-storage (Tank-in-tank) | Total volume 0.725 $m^3$, inner domestic water tank 0.175 $m^3$, 5 ports |
| Heat pump | HGX 12P/110-4s, heating capacity 3-12 kW, R134a |
| Circulation pump | P1: NMT PLUS 25/80-180, IMPPUMPS<br>P2: UPS 25-40-180,Grundfos<br>P3: UPS 25-60-180, Grundfos<br>P5:Alfa 125-60-180,Grundfos<br>P6:Magna 25-60-180,Grundfos |
| Horizontal ground heat exchanger | HDPE pipe, 240 m; Cover area 8.5 m x 30 m |
| Controller | LMC 320 for the auxiliary loop; UVR63 for the solar collector loop |

The solar collectors are Thermomax HP 450 evacuated tubular collectors from Kingspan, designed specifically for higher latitude climates. The collectors provide heat even in cold or windy climate conditions. The efficiency expression of the collectors is given in the following equation [19 20]:

$$\eta = 0.75 \cdot k_{IAM} - \frac{1.18 \cdot (T_m - T_a)}{G} - \frac{0.01 \cdot (T_m - T_a)^2}{G} \quad (1)$$

where $k_{IAM}$ is the incidence angle modifier, detailed information on the incidence angle modifier of the collectors can be found in [20]; Tm is mean solar collector fluid temperature, °C; $T_a$ is ambient air temperature, °C; and G is the solar irradiance, W/$m^2$.

The solar collectors were installed on a south-facing roof with a tilt of 45°, which provided heat for two parallel loops respectively coupled to the combi-storage and to the HGHE using two flat plate heat exchangers. Solar energy is directly supplied to the combi-storage via one flat plate heat

exchanger, and the ground loop in regenerative mode is constructed with HGHE connected to the solar collectors via another one. Each plate heat exchanger has an overall heat transfer area of 0.5 $m^2$ and a capacity of 9 kW. The capacity of the heat exchanger is much higher than the maximum power of the solar collectors (approx.. 6 kW). The solar collector fluid is an antifreeze solution with 35% propylene glycol and 65% water. A mixture of 35 % isopropyl alcohol (IPA) and 65 % water was used as heat transfer fluid in the HGHE.

A single stage piston compressor was selected as the core component of the heat pump, and integrated in the heat pump cabinet together with two circulation pumps (P5 and P6). The compressor was designed to operate on a nominal compressor frequency of 50 Hz in on/off mode. In the modulating mode, the frequency inverter allows the compressor to be operated with a frequency between 30 Hz and 70 Hz. The power consumption of the compressor is a function of the compressor frequency with higher frequency for higher power. The frequency inverter allows the heat pump to alter the compressor power in order to satisfy the heating demand.

A big uninsulated buffer tank and a cooling system combined with an insulated storage tank acted as heat sink for both the SH loop and the DHW loop. Automated draw offs of DHW were made three times a day to simulate an actual demand in a single-family house. The volume flow rate during tapping was around 7.5 l/min. In total, a DHW consumption of approximate 5 kWh was tapped every day. For SH during the heating period, heat was drawn from the combi-storage every day in predefined time slots that varied from month to month. The volume flow rate was around 5 l/min. The yearly space heating demand was about 2800 kWh.

## *2.2 Operation and control*

In the SGHP system, the UVR 63 controller from Technische Alternative was used to control the solar collector loop to switch between the combi-storage and the ground loop. The auxiliary heating loop system was controlled by the controller LMC 320 from Lodam electronics. A detailed description of the control strategies is shown in Table 2.

**Table 2** Control strategies of the SGHP system

| Location | Function | Controlling strategy | Implementation process |
|---|---|---|---|
| | Heating for the combi-storage | TA1> TA2 + 8 K & TA1> 20°C & TA2 <65°C | P1+M7+M2+P2 |

| | | | |
|---|---|---|---|
| The solar collector loop | Charging for HGHE (Regeneration mode) | TA1> TA3 + 8 K & TA1> 20℃ & TA3 <30℃ | P1+M7+P3 |
| The auxiliary heating loop | Heating for DHW (Top) | T3<Tset-4 K until T3>Tset; Tset=51℃ (47℃≤T3≤51℃) | P5+P6+HP+M6+M5 |
| | Heating for SH (Middle) | T6<Tset-5 K until T6>Tset; Tset=31℃ (26℃≤T6≤31℃) | P5+P6+HP+M6+M4 |
| SH loop | Heating for space | Heat demand/flow temperature | Setting time switch, M8 |
| DHW loop | DHW | Three time operation every day | Setting time switch |

For the solar collector loop, the temperature sensor in the upper part of the solar collector panel (TA1), the temperature in the tank (TA2) and the temperature in the ground (TA3) were used to control operation of the circulation pump P1, P2 and P3 and to evaluate whether the combi-storage or HGHE should be charged. When TA1 is 8 K higher than water temperature TA2 in the bottom of the combi-storage, the combi-storage will be charged by adjusting the motorized valves M7/M2 and activating the circulation pump P1 and P2. The charging process will be stopped when the temperature difference between TA1 and TA2 was lower than 2 K. Similarly, the HGHE will be charged by adjusting the motorized valve M7 and activating the circulation pump P1 and P3 when TA1 is 8 K higher than the outlet fluid temperature of HGHE (TA3). The charge of the HGHE will continue until the temperature difference between TA1 and TA3 is lower than 4 K. It should be noted that the combi-storage and HGHE could not be charged at the same time.

For the auxiliary heating loop, the heat pump operation status is controlled by the temperature sensors (T3/T6). The 3-way motorized valve (M6) directs heat from the heat pump either to the DHW part or to the SH part of the combi-storage depending on measured temperatures of the sensors (T3/T6). The measured T3 and T6 is respectively compared to the setting point temperatures for DHW ($T_{set}$=51℃) and SH ($T_{set}$=31℃), and the controlling temperature difference is set 4 K for DHW and 5 K for SH. For example, when T3 is lower than 47℃, the valves M6/M5 are adjusted and circulation pumps (P5 and P6), heat pump are activated, consequently the upper part of the combi-storage is continuously heated until the temperature reaches 51℃. In this way, the water temperature in the upper part of the inner tank was kept within the range of 47℃-51℃. Similarly, the water temperature of SH volume is kept within the range of 26℃-31℃ by switching M6/M4 and activating pumps (P5 and P6) and the heat pump. Similar to the way motorized valve M7 works, M6 is used to switch for the charge of the DHW volume or the SH volume.

The presented SGHP system was tested under real weather conditions in 2019 except five days of break due to power failures, including one day in March and 4 days in July. The energy flows of the SGHP system and its main components were analyzed in the 360 days, and thermal performance of the SGHP system was evaluated based on the measured energy flows and electricity consumption.

## *2.3 Measurement system*

### *2.3.1 Measurement description*

The temperatures at different key locations, the volume flow rates of the different loops and electricity consumption of different components were measured and logged at an interval of 1 minute. The ambient air temperature, the indoor temperature in the test facility and the total solar radiation on the solar collectors were also measured at the same time. A detail distribution of the monitoring sensors was shown in Fig.2.

For the temperature sensors, the points marked in green (TA1—TA4) were used for control of the solar collector loop. The points marked in black (T1—T9) were used for control of the heat pump system and for safety operation of the piston compressor. The other sensors (orange mark points) were all used for monitoring the key temperatures and volume flow rates to calculate the dynamic thermal performance of the different loops.

For the HGHE, the HDPE pipe outside diameter and wall thickness are respectively 40 mm and 2.5 mm, and the total pipe length is 240 m. The whole surface area of HGHE was exposed to solar radiation during the day, and temperature sensors located in two lines perpendicular to the flow direction were set to measure the ground temperatures respectively in the level of the hoses, 0.5 m above the hoses and 0.5 meter below the hoses. At the same time, the ground temperatures were measured vertically below the hoses with an interval of 1 m and a total depth of 10 m for two locations: B2 right next to the HGHE, and B1 10 m away from edge of the HGHE. The sensors at B1 were used to measure the undisturbed ground temperature. The locations and numbering of all sensors were shown in Fig.3.

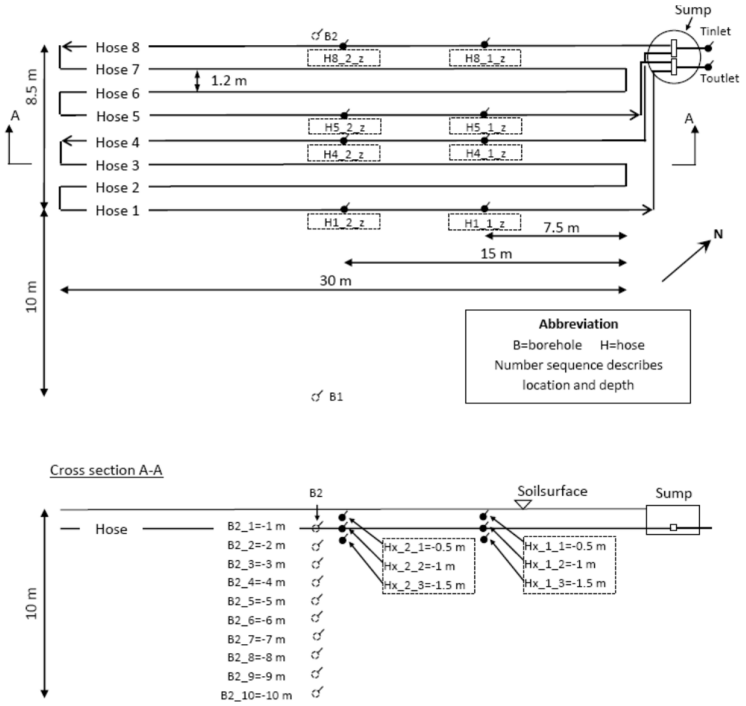


**Fig.3** The schematic illustration of HGHE with all measurement points

*2.3.2 Measurement equipment*

A National Instrument cRIO with 9214 and 9403 cards was used for the data logging. The total and diffuse irradiances on the same plane as the tilted collectors were measured using CMP11 Kipp & Zonen pyranometer. All temperature sensors were Type TT thermocouples (Copper/Constantan), and the different flow sensors were applied in the different loops. The electricity consumptions of the different loops were also measured in the SGHP system. Table 3 showed the measurement equipment and measurement uncertainty. The flow meter and electricity energy meter were shown in Fig.4. The energy quantities in the loops are determined from measured temperatures and volume flow rates, and it is estimated that the accuracy of the measured energy quantities are within 5 %. The electricity consumption is measured with energy meters, and it is estimated that the accuracies of the measured electrical energy quantities are within 0.5 %.

**Table 3** The measurement equipment

| Equipment | Type | Location | Accuracy |
|---|---|---|---|
| Flow sensor | Brunata HGS5-R4 | Ground loop/F6 | ± 1 % |
| | Brunata HGQ1-R0 | Solar heating for the combistorage/F2 | ± 2 % |
| | Brunata HGQ1-R3 | The auxiliary heating loop/F5 | ± 2 % |
| | Brunata HGQ1-R0 | SH loop/F3 | ± 2 % |
| | Clorius Combimeter 1.5 EPD | DHW loop/F7 | ± 2 % |
| Temperature sensor | Copper/constantan, type TT | System | ± 0.5 K |

| | | | |
|---|---|---|---|
| Energy meter | Malmbergs 09 815 51/ Kamstrup | Different loop | ± 0.5 % |


**Fig.4** The flow meter and electricity energy meter

## 3. Analysis method

For the SGHP system, analysis of energy balance and thermal performance is essential for a deep understanding of the system under the given operating conditions. The power input and output in the different loops can be calculated by the following equation:

$$\dot{Q} = \rho V c_{\mathrm{p}} (T_{\mathrm{in}} - T_{\mathrm{out}}) \tag{2}$$

Where the dependence of water dynamic physical parameters on temperature can be described as follows[38]:

$$\rho(T) = 1000.6 - 0.0128T^{1.76} \tag{3}$$

$$c_{\mathrm{p}}(T) = 4209.1 - 1.328T + 0.01432T^{2} \tag{4}$$

For the physical parameters of IPA mixture fluid in the ground loop, $\rho_{\mathrm{mix}} = 925$ kg/m$^3$ and $c_{\mathrm{mix}} = 3.71$ kJ/(kg ℃) is respectively applied in the analysis and calculation of energy flow.

Efficiency is one of the main performance indicators for heating and cooling systems and is generally defined as the ratio between the useful energy output from the system to the energy input to the system. $SPF_{\mathrm{SHP}}$ is mainly used as a system performance indicator for the SGHP system,

which can be calculated for a given period. The useful energy output is the load of SH and DHW, and final electrical energy consumption is considered as energy input. The $SPF_{SHP}$ is given as:

$$SPF_{SHP} = \frac{\int (\dot{Q}_{SH} + \dot{Q}_{DHW})\mathrm{d}t}{\int (\sum \dot{E})\mathrm{d}t} \tag{5}$$

Where $\dot{Q}_{SH}, \dot{Q}_{DHW}$ is respectively the heat flow rate of space heating and domestic hot water, kW, $\dot{E}$ is the electricity power of the different components, kW; and $t$ is the integration time for energy flow calculation, h.

For the auxiliary heating loop, the performance of the heat pump system with HGHE and the heat pump can be evaluated using $SPF_{HP+HS}$ and $SPF_{HP}$:

$$SPF_{HP+HS} = \frac{\int (\dot{Q}_{HP})\mathrm{d}t}{\int (\dot{E}_{HP} + \dot{E}_{P5} + \dot{E}_{P6})\mathrm{d}t} \tag{6}$$

$$SPF_{HP} = \frac{\int (\dot{Q}_{HP})\mathrm{d}t}{\int (\dot{E}_{HP})\mathrm{d}t} \tag{7}$$

Where $\dot{Q}_{HP}$ is the heat flow rate of the auxiliary heating loop, kW; $\dot{E}_{HP}, \dot{E}_{P5}, \dot{E}_{P6}$ is respectively the electricity power of heat pump, pump P5 and pump P6, kW.

In order to evaluate the share of solar energy delivered to the combi-storage in SGHP system, solar fraction shown in Eq. (8) is used to calculate the ratio of direct solar heat to the useful heat. The solar fraction has a value in between 0 and 1. A fraction of 1 indicates completely coverage of heat demand by solar energy and there is no auxiliary heat needed. The solar fraction is zero if the solar input is lower than the heat loss from the systems [2].

$$f_{sol} = \frac{\int (\dot{Q}_{sol})\mathrm{d}t}{\int (\dot{Q}_{DHW} + \dot{Q}_{SH})\mathrm{d}t} \tag{8}$$

For the SGHP system using solar energy and ground heat energy, the solar fraction does not reflect the full potential of the system to use renewable energy sources, the exploiting efficiency of renewable energy can be expressed by the renewable heat fraction. It is defined as,

$$f_{\mathrm{re}} = 1 - \frac{\int (\sum \dot{E}) \mathrm{d}t}{\int (\dot{Q}_{\mathrm{SH}} + \dot{Q}_{\mathrm{DHW}}) \mathrm{d}t} = 1 - \frac{1}{SPF_{\mathrm{SHP}}} \tag{9}$$

# 4. Results and discussion

Based on the monthly energy flows from the input and heating demand, the energy balance in the combi-strorage and the monthly $SPF_{\mathrm{SHP}}$ are analyzed in section 4.1.1, and the contributions of solar energy and ground heat source are respectively shown. Section 4.2.1 describes the solar energy flows for heating the combi-storage and charging the ground in regeneration mode, and the monthly ground charging/discharging energy flow are discussed in section 4.2.2. Furthermore, system performance for application of renewable energy source are evaluated by use of the monthly solar fraction and renewable heat fraction in section 4.3. Fig.5 outlines the interactive relations of the different section.

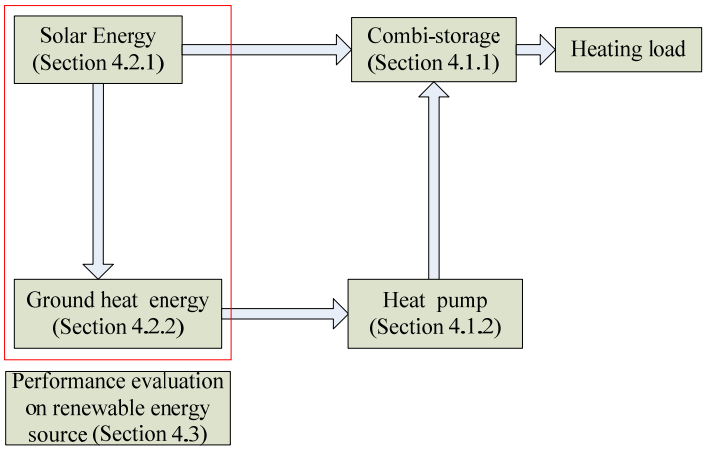


**Fig.5** The flow chart of the interactive relations of the different section in the discussion.

## *4.1 Monthly operation performance of the SGHP system over the year*

### *4.1.1 Energy balance and SPF*$_{SHP}$

Based on the measured electricity consumption and energy flows, monthly heat demand was obtained and an energy balance analysis was carried out. For the GSHP system, the energy balance for is presented as the following equation:

$$Q_{sol} + Q_{HP} + Q_{ec} - (Q_{DHW} + Q_{SH}) - Q_{heat.loss} = 0 \quad (10)$$

where $Q_{sol}$ is the heat flow to the thermal storage by the solar collectors, kWh; $Q_{HP}$ is the heat flow from heat pump, kWh; $Q_{ec}$ is energy change of the storage, kWh; and $Q_{heat.loss}$ is the monthly heat loss of GSHP system, kWh. In Eg. (10), the heat loss $Q_{heat.loss}$ includes heat loss from the combi-storage and heat loss from the connection pipes between the heat pump and the combi-storage. Since it is difficult and complex to measure these heat losses directly, $Q_{heat.loss}$ is obtained by the energy balance equation.

Fig.6 illustrates the monthly energy flows of the system. The positive values are the energy input of the system, while the negative values are the energy output of the SGHP system, and average monthly energy change in the storage is shown as $Q_{ec}$. The tank temperature $T_{tank}$ is mass weighted average temperature of the tank based on measurement of the temperature sensors T25-T32 as shown in Fig. 2(a). The average monthly water temperature in the combi-storage $T_{tank}$ and the outdoor air temperature $T_a$ are shown in Fig. 6 as well.

As shown in Fig. 6, the average hot water temperature in the combi-storage was higher than 32 °C from January to March and from November to December, even though the ambient air temperature was lower than 7 °C. For the ground loop, its contribution for heating, shown as Q(ground to HP) in Fig. 6, was larger than the direct solar energy in these five months. In April of the highest radiation, the monthly average hot water temperature in the combi-storage is largely determined by solar charge for the combi-storage where auxiliary heat was hardly needed except for cloudy or rainy days. At the same time, the heat demand decreased to the level of DHW load after the space heating was stopped on 3, April. Therefore, the clear and cloudless weather conditions

and the lower heat demand caused the monthly average hot water temperature in the combi-storage increased up to the yearly maximum temperature of 63 °C when surplus solar heat was stored in the combi-storage, and the corresponding $Q_{heat.loss}$ was highest.

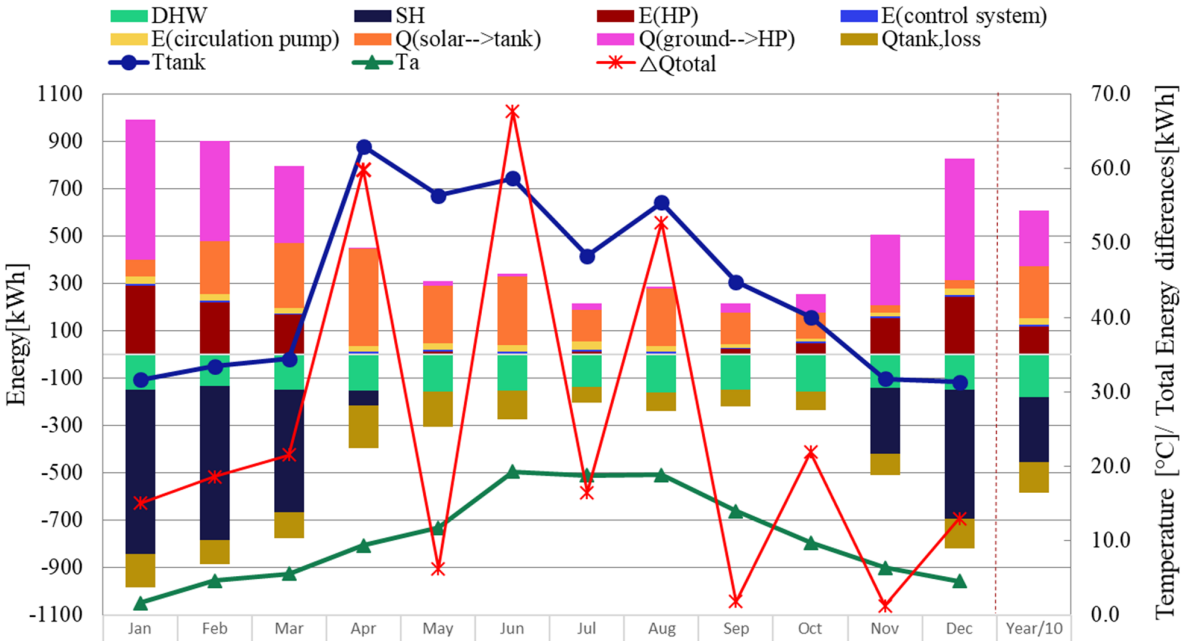


| | Jan | Feb | Mar | Apr | May | Jun | Jul | Aug | Sep | Oct | Nov | Dec | Year/10 |
|---|---|---|---|---|---|---|---|---|---|---|---|---|---|
| Qtank,loss | -140.3 | -104.1 | -109.6 | -179.0 | -150.1 | -124.2 | -67.6 | -78.5 | -69.1 | -79.0 | -90.8 | -125.2 | -131.8 |
| Q(ground-->HP) | 593.4 | 424.9 | 324.7 | 6.7 | 21.5 | 12.1 | 27.9 | 9.9 | 39.1 | 79.8 | 299.8 | 513.4 | 235.3 |
| Q(solar-->tank) | 71.9 | 223.2 | 272.9 | 410.6 | 243.0 | 290.1 | 134.1 | 241.0 | 136.3 | 108.6 | 28.6 | 34.3 | 219.5 |
| E(circulation pump) | 30.2 | 26.5 | 23.5 | 24.0 | 27.1 | 26.7 | 36.2 | 25.0 | 12.9 | 10.5 | 18.1 | 27.6 | 26.1 |
| E(control system) | 7.1 | 6.4 | 6.9 | 6.9 | 7.1 | 6.9 | 6.2 | 7.1 | 6.9 | 7.1 | 6.9 | 7.1 | 7.6 |
| E(HP) | 291.4 | 221.1 | 168.0 | 4.4 | 11.8 | 4.9 | 12.6 | 4.3 | 22.2 | 48.9 | 153.3 | 244.6 | 118.8 |
| SH | -694.6 | -650.4 | -519.1 | -63.2 | 0.0 | 0.0 | 0.0 | 0.0 | 0.0 | 0.0 | -276.1 | -545.2 | -274.8 |
| DHW | -149.4 | -133.3 | -148.5 | -153.2 | -157.0 | -151.5 | -135.4 | -158.8 | -149.3 | -154.7 | -141.6 | -149.5 | -178.2 |
| Ttank | 31.6 | 33.4 | 34.4 | 63.0 | 56.4 | 58.7 | 48.3 | 55.5 | 44.8 | 40.0 | 31.7 | 31.3 | |
| Ta | 1.6 | 4.6 | 5.5 | 9.3 | 11.7 | 19.3 | 18.8 | 18.8 | 13.9 | 9.7 | 6.3 | 4.5 | |
| △Qtotal | 15.0 | 18.6 | 21.5 | 60.0 | 6.2 | 67.7 | 16.4 | 52.8 | 1.8 | 21.9 | 1.2 | 13.0 | |

**Fig.6** Monthly heat demand and energy balance over the year

Solar energy was the dominant heat source from April to September when solar radiation was higher. The active solar input (positive value) was much larger than the heating load, which resulted in an increase of the average hot water temperature and enlarged $Q_{ec}$.

Heat loss from the tank is determined by insulation of the tank and the temperature difference ($T_{tank}$-$T_{ia}$) between the tank and the indoor aor. The temperature difference ($T_{tank}$-$T_{ia}$) in summer is larger than those in other seasons. Especially for April, the maximum $Q_{heat.loss}$ was up to 200 kWh corresponding to a high temperature difference of 44.5 °C. Ttank reached the maximum of 63 C in

April due to higher solar radiation and lower heat demand, therefore heat loss from the tank was the highest. For the yearly heat losses of the combi-storage $Q_{heat.loss}$, it amounted for about 120 kWh/month in average, which corresponds to 24 % of the amount of heat charged to the storage or 76 % storage efficiency. The higher $Q_{heat.loss}$ could be explained by the following reason: a) The heat loss from the tank is influenced by insulation of the tank and by the temperature difference ($T_{tank}$-$T_{ia}$). The tank is insulated with 200 mm, 50 mm and 0 mm mineral woll on the top, the side and the bottom of the tank. Poor insulation of the tank bottom results in higher heat loss from the tank. b) The heat loss from the connection pipe depends on insulation of the pipe and the operation conditions. Poor insulation of the pipes and frequent on/off of flow in the pipes result in higher pipe heat loss.

The monthly $SPF_{SHP}$ of the SGHP system and the average daily total solar radiation on the collector surface are shown in Fig. 7.

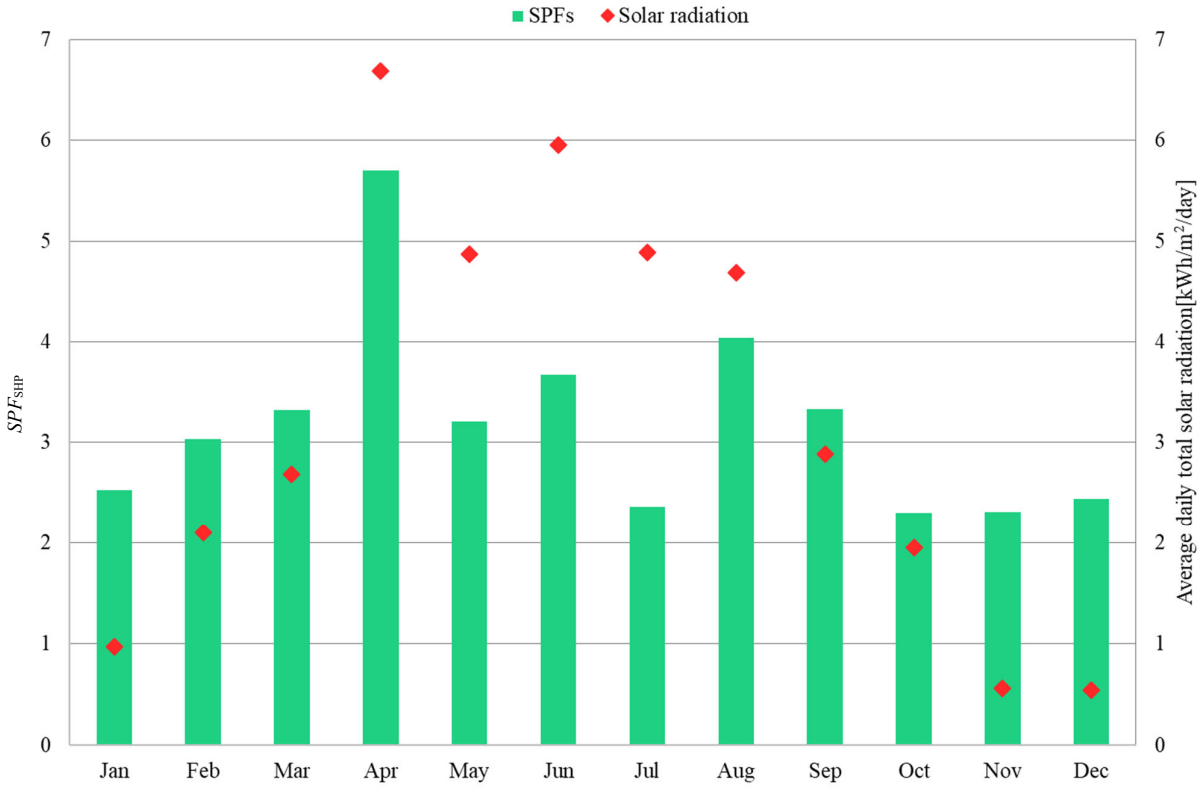


**Fig.7** Average daily total solar radiation on solar collectors and the monthly $SPF_{SHP}$ of the SGHP system

As shown in Fig. 7, the $SPF_{SHP}$ in the seven months were all higher than 3, and the yearly $SPF_{SHP}$ was 2.83. The daily total solar radiation was higher than 4.5 kWh/m$^2$/day from April to August, and the yearly average value was 3.2 kWh/m$^2$/day. For the period from January to April, an increase of the solar energy share and a decrease of the ground heat energy share were observed in Fig. 6 due to an increase of solar radiation. The maximum $SPF_{SHP}$ (5.7) was achieved in April with the highest solar radiation (6.7 kWh/m$^2$/day). In the last four months of the year (from September to December) shown in Fig. 6, the share of ground heat energy increased obviously with the decrease of solar radiation and the increase of heat demand. The minimum $SPF_{SHP}$ (2.3) was obtained in November. In the six months with only heating for DHW (from May to October), the variation of the $SPF_{SHP}$ was mainly dependent on solar radiation. The power failures in four days of July resulted in more electricity consumption of heat pump and circulation pumps, which significantly decreased $SPF_{SHP}$ even in the period with higher solar radiation.

*4.1.2 Heat pump performance*

Fig.8 illustrates the monthly performance of the heat pump system. The electricity consumption of the heat pump system increased obviously when solar radiation was lower than 4 kWh/m$^2$/day in the period from January to March and from September to December. The lower the solar radiation, the higher the electricity consumption of the heat pump system will be. In five months with heat demand for DHW and SH (from January to March and from November to December), more heating demand required the heat pump operation continuously, and the $SPF_{HP}$ was still higher than 3 though the electricity consumption of the system increased.

In the spring-summer period from April to August, the monthly average solar radiation was higher than 4 kWh/m$^2$/day. The heat pump system started occasionally in cloudy or rainy days. The lowest ground temperature caused by continuous heat extraction from January to March resulted in the lowest $SPF_{HP+HS}$ (2.4) in April. The $SPF_{HP+HS}$ was improved by 38% from April to June with continuous charge of the ground, and kept higher than 2.9 due to the higher ground temperature even though the heat pump system seldom started from May to August. The yearly $SPF_{HP+HS}$ and

$SPF_{HP}$ were respectively 2.8 and 3.1 in 2019, which illustrated that the heat pump system was successful in applying ground heat energy as the supplemental heat source in the period of low solar radiation.

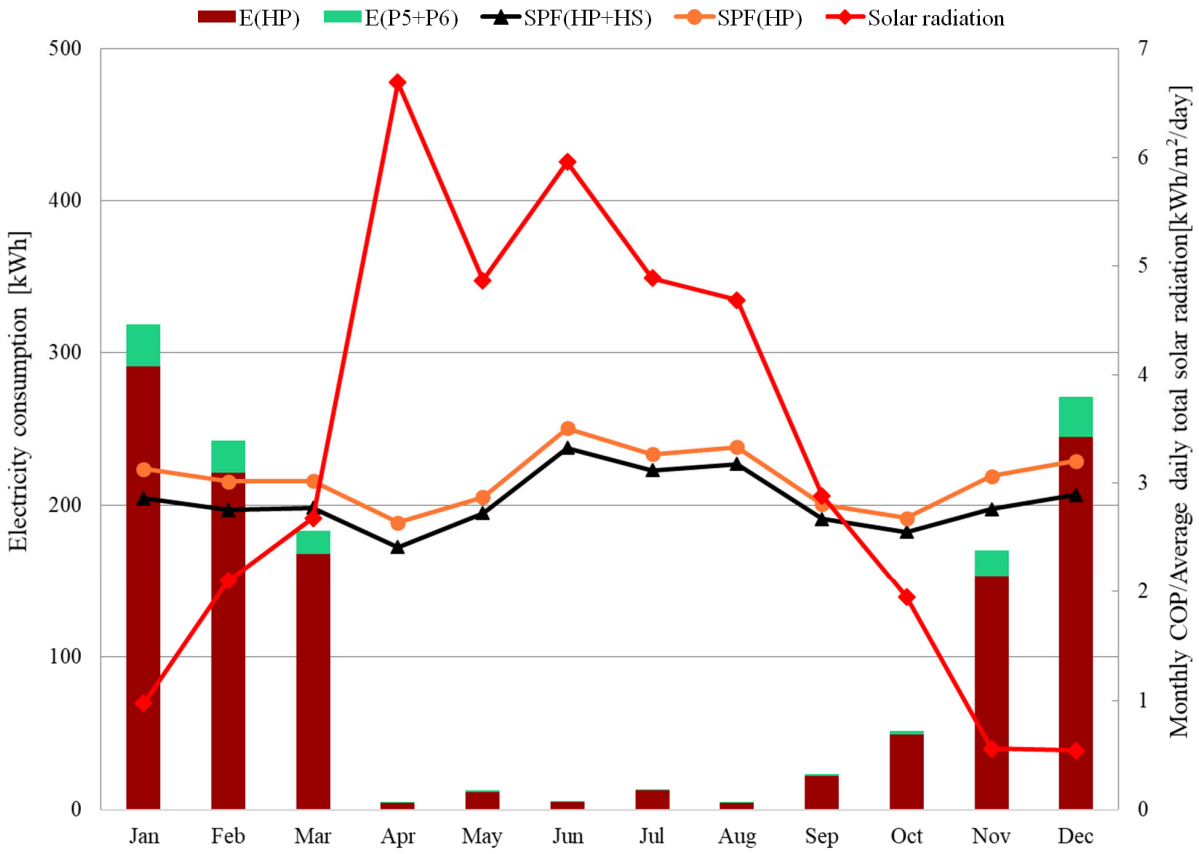


**Fig.8** The electricity consumption and the monthly $SPF_{HP+HS}$ of the heat pump system

## *4.2 The dynamic performance of the system*

### *4.2.1 Solar energy flow*

The total input of yearly solar energy for the SGHP system was 4879 kWh in 2019. Fig.9 shows monthly average daily solar radiation and utilization of solar energy. The solar heat used to charge the combi-storage is shown as the red bar, while the heat to charge the ground is shown as the blue bar. As shown in Fig.9, the maximum used solar energy was 862 kWh in April, and the minimum was only 40 kWh in November. It was observed that the monthly used solar energy was higher than 500 kWh when the solar radiation was larger than 4.7 kWh/m$^2$/day from April to August.

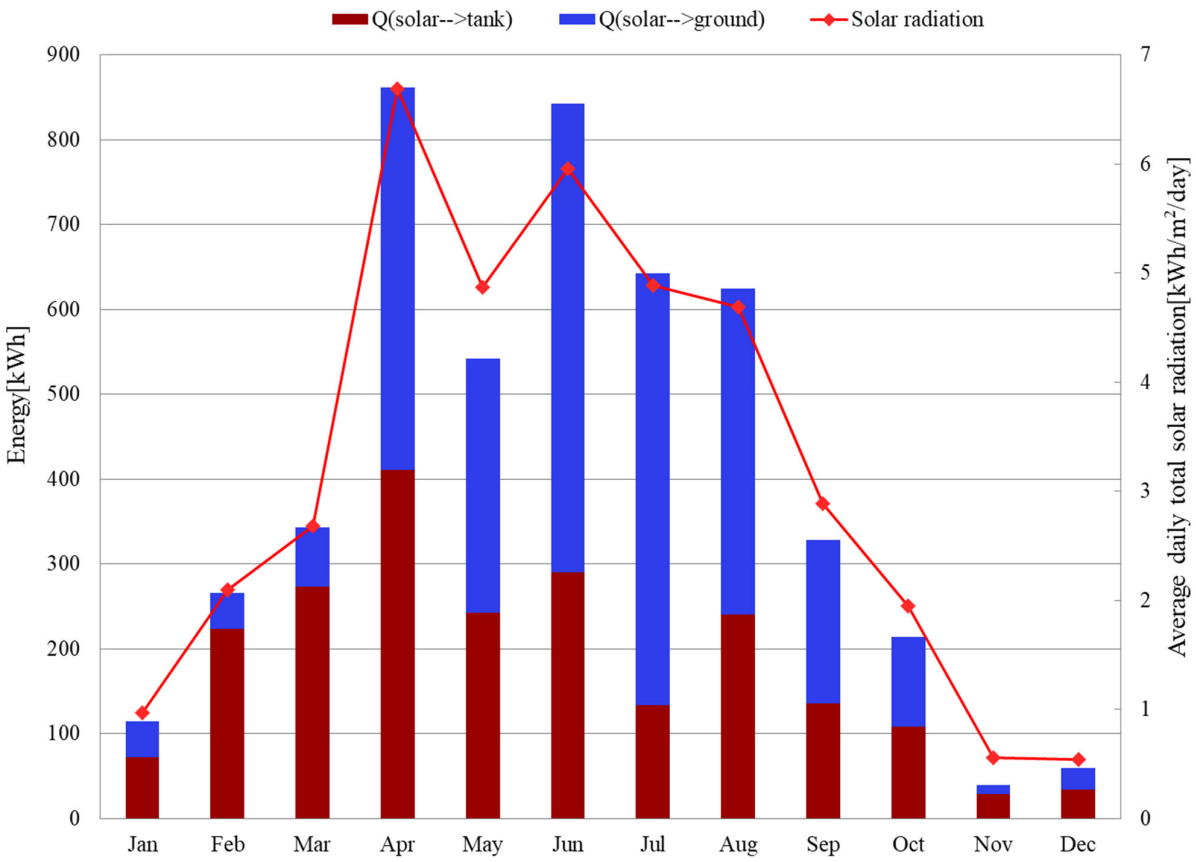


**Fig.9** The solar radiation and monthly utilization of the produced solar heat in 2019

As shown in Table 2, solar heat was used to charge either the combi-storage or charge the ground based on the setting temperature difference. In the winter months from January to March and from November to December, solar heat was mostly used to charge the combi-storage, which provided heat to cover the demand for DHW and SH. Since the heat demand was high and solar energy was limited in winter, the first priority for the produced solar heat was direct utilization. In December with the lowest solar radiation, the useful direct solar energy accounted for 58% of the total solar heat production.

Under the premise that the combi-storage was fully heated in the period with higher solar radiation than 4 kWh/m$^2$/day, excess solar energy would be diverted to charge the ground to improve $SPF_{HP+HS}$ of the heat pump system. In April with the highest $SPF_{SHP}$, solar heat of more than 400 kWh was directly utilized to cover the demand for DHW and SH, and solar heating of 450 kWh was used to charge the ground in the regeneration mode. Generally, the annual solar energy

used for charge of the ground accounted for 55% of heat produced by the solar collectors, and it was nearly 500 kWh higher than the directly utilized solar energy over the year.

*4.2.2 Ground charging/discharging energy flow*

The HGHE works as a heat source in the heat pump system and as a heat sink in the regeneration mode, and the thermal performance of the HGHE is also strongly influenced by solar radiation on the ground surface. 2353 kWh of ground heat energy was extracted for the combi-storage by heat pump system in 2019, which was lower than yearly solar energy charging for the ground. Monthly energy flow from/to the ground is shown in Fig.10. For the ground, the maximum net energy output was 550 kWh in January, and 593 kWh of ground heat energy was charged for the combi-storage. In June, only 12 kWh was extracted from the ground, the maximum value of net energy input was up to 555 kWh due to the highest solar energy charging for the ground.

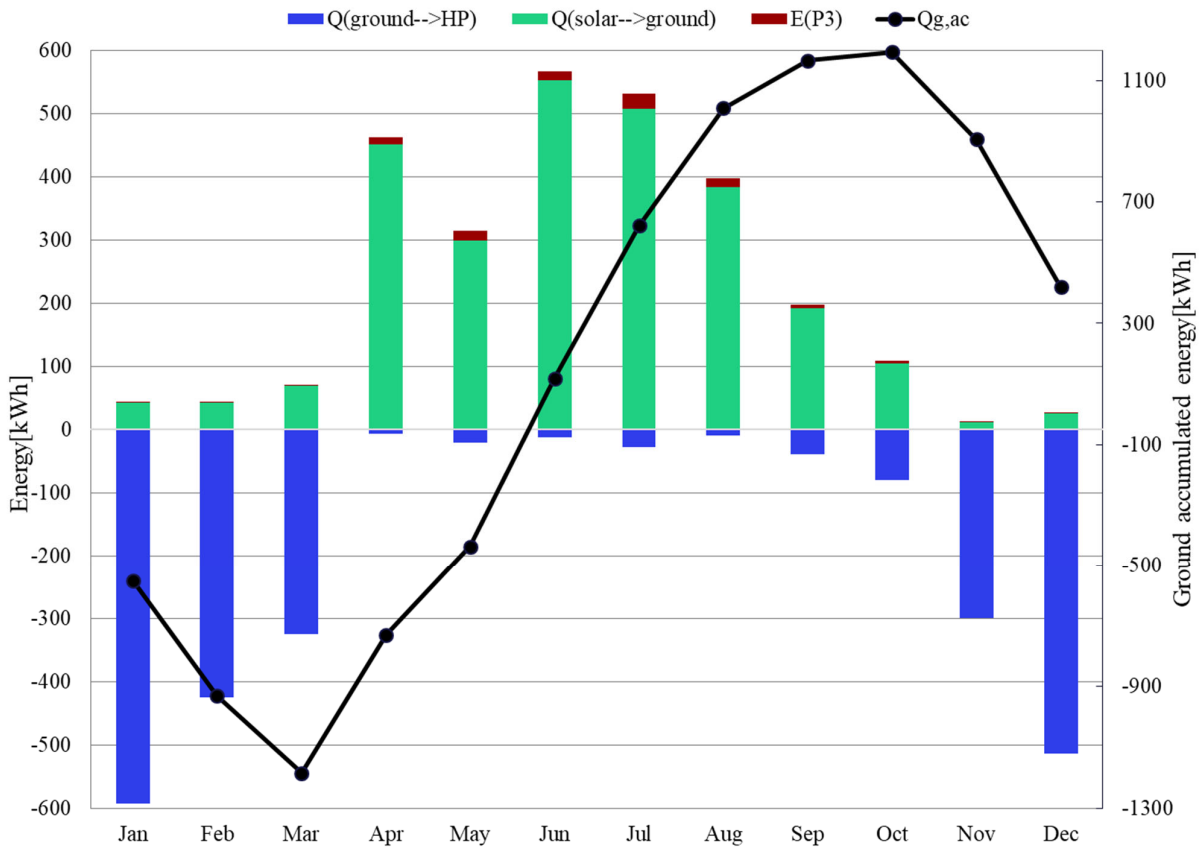


**Fig.10** The monthly energy flow of charging/discharging ground

In the SGHP system, the operation role of the HGHE can be automatically adjusted many times a day, depending on the temperature differences as shown in Table 2. It was observed in Fig.10 that the heat input into the ground was higher than that taken from the ground from April to October, while the opposite occurred for the other five months of the year. The ground heat accumulation $Q_{g,ac}$ from start month to the current month was monthly calculated by summarizing the monthly net heat inputs over the year and shown in Fig.10. The ground accumulated energy dropped to the lowest value in the first three months due to continuous discharge of the ground. Starting in April, more solar heat was used to charge the ground due to a higher solar radiation and a lower heat demand. The ground accumulated energy peaked at approximate 1200 kWh in October. Afterwards it started to decline due to discharge of heat from the ground via the heat pump system, until in December the ground accumulated energy dropped to 410 kWh. A positive accumulated energy at the end of the year means that there was surplus solar heat charged to the ground compared to the heat taken from the ground by the heat pump system.

For the heat pump system, its electricity consumption is sensitive to the ground temperature. A surplus of heat into the ground will increase the temperature of the soil and therefore improve the thermal performance of the heat pump. As shown in Fig.8, the $SPF_{HP+HS}$ in the last three months of the year kept increasing even with an increase of the heating demand, which was most likely due to continuous charging of the ground over the year. Undoubtedly, a positive ground heat accumulation will improve operating performance of the SGHP system in the next year.

### *4.3 System performance evaluation on renewable energy source*

In addition to the $SPF_{SHP}$ for the SGHP system and the $SPF_{HP+HS}$ for the heat pump system, solar fraction is used to evaluate solar contribution to the overall energy output of the SGHP system. Considering the two renewable energies used in the SGHP system, a renewable heat fraction is also calculated to reflect the potential of renewable energies. The solar fraction $f_{sol}$ and the renewable heat fraction $f_{re}$ are respectively defined using EQs (8) and (9), and the monthly solar fraction and renewable heat fraction in 2019 are shown and compared in Fig. 11. As shown in Fig. 6 and Fig. 7,

from April to August, there was a lower heating demand and a higher solar radiation, resulting in solar fractions higher than 0.65. The highest solar fraction was up to 0.95 in April with the highest solar irradiation, while the lowest solar fraction was only 0.15 in October when the solar radiation was larger than 1.8 kWh/m$^2$/day. However, the solar fraction was zero in the three months (January/November/December).

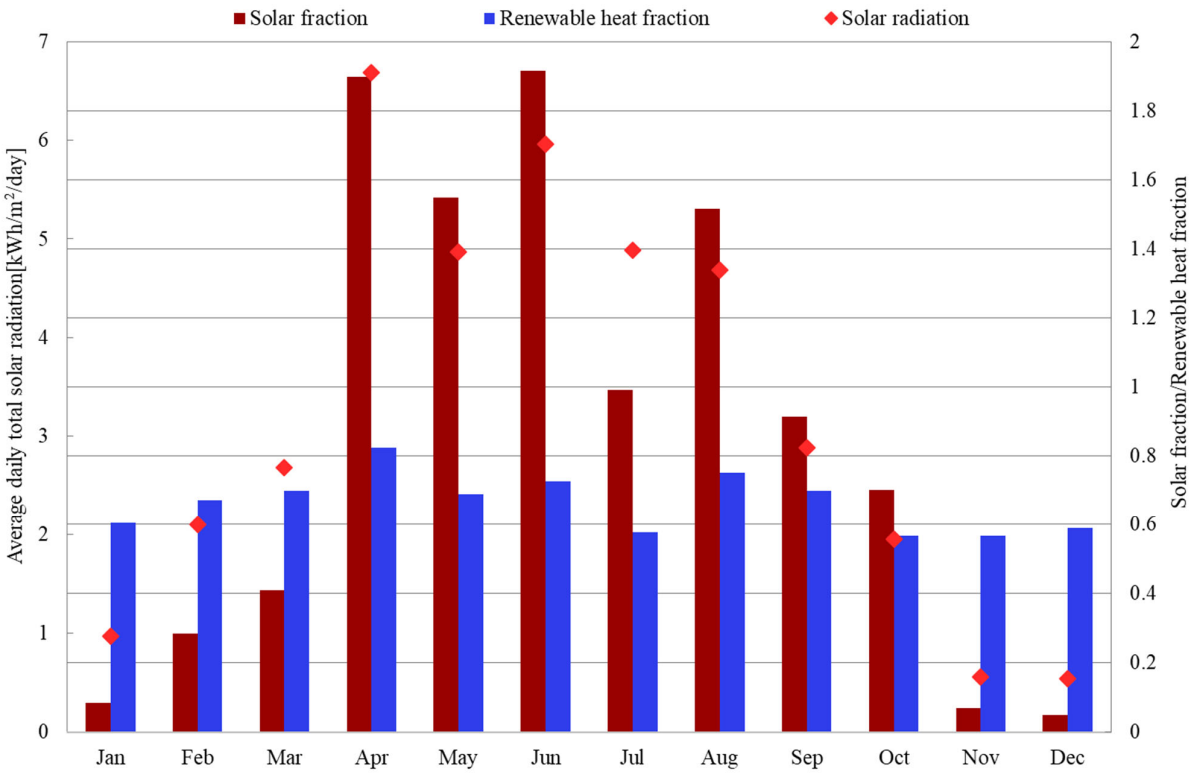


**Fig.11** The monthly solar fraction and renewable heat fraction

Different as the dramatic fluctuation of the solar fraction, a less fluctuating renewable heat fraction defined by Eq. (9) is shown in Fig.11. The relative difference between the highest value in April and the lowest value in October is 31%. A supplement of ground heat energy made operation of the SGHP system more stable and robust against seasonal fluctuations of solar energy resources, which is considered essential for heating of a single-family house using renewable energies. The annual renewable heat fraction reached 65%, which shows potential of SGHP system for DHW and SH for a single-family house.

### *4.4 Discussion*

The experimental results revealed the dynamic characteristic and monthly energy flows of the SGHP system. Higher $SPF_{SHP}$ and renewable heat fractions were achieved. However, the component sizes and control strategy of the SGHP system were not optimal, the pipe lengths and sizes in the lab system also caused significant extra energy losses, which reduced the performance of the system. In addition, the hot water in the combi-storage needed to be heated to the normal level by the heat pump system under the condition of low solar radiation and night, which resulted in an increase of electricity consumption with the discharge of heat. More efforts should be made to improve the system performance by optimizing the component sizes and control strategies based on further experimental and theoretical investigations.

## 5. Conclusions

By combining solar collectors and heat pump system with HGHE, operation instability of the SGHP system caused by fluctuating weather conditions was minimized with an increased utilization efficiency of solar energy. The efficiency and operation performance of the heat pump system will increase due to a higher soil temperature. Detailed experimental investigations were carried out on a SGHP system for a single-family house in Denmark. The following conclusions are drawn:

1) For the SGHP system, directly utilized solar energy accounted for 36.6% of annual heat input of the combi-storage, the rest of the heat was supplied by the heat pump system that consumed 84% of the annual electricity consumption of the SGHP system. The annual $SPF_{SHP}$ was 2.8, and the maximum monthly $SPF_{SHP}$ was up to 5.7 in April with the highest solar radiation.
2) Besides the direct utilization, heat produced by the solar collectors was also used to charge the ground, which decreased operation temperature of the solar collectors and thus increased the efficiency of the solar collectors. The annual solar heat charged in the ground accounted for 55% of heat produced by the solar collectors, and it was 500 kWh higher than the annual solar heat directly utilized.

3) With heat taken from the ground, operation of the heating system becomes more stable and robust against seasonal fluctuations of solar energy resources. The $SPF_{HP+HS}$ of the heat pump system decreased to 2.4 in April after 3-month continuous heating extraction from the ground. Even though there was a continuously increasing heating demand since October, the $SPF_{HP+HS}$ increased up to 2.9 in December due to the surplus solar heat stored in the ground during the summer. The annual $SPF_{HP+HS}$ of the heat pump system was 2.8 for 2019.
4) Although the solar fraction varies from month to month due to fluctuations of solar energy resources, the system can still achieve a rather stable renewable energy fraction. The monthly solar fractions are all higher than 0.65 from April to August, and the highest solar fraction $f_{sol}$ is up to 0.95 in April with the highest solar radiation in 2019. The annual renewable energy fraction $f_{re}$ was up to 0.65, and the monthly $f_{re}$ were all higher than 0.56 in the three months (January/November/December) with lower solar radiation.

As a future work, the experimental investigation will be used to validate the model of SGHP system and different component model. Using the validated system model, the system performance and the control strategy can be effectively evaluated under different weather condition, and the optimization on the sizes of system components and control strategy will be focused based on the characteristics of the heating demands.

## Acknowledgements

This work was financially supported by Bjarne Saxhofs foundation, the Overseas Visiting Scholars Project of Shandong University of Science and Technology (2018), and the National Science Foundation of Shandong Province (ZR2020ME187).

## References

[1] Energy consumption in households. https://ec.europa.eu/eurostat/statistics-explained/index.php/Energy_consumption_in_households.

[2] Hadorn J-C. Solar and heat pump systems for residential buildings. John Wiley & Sons; 2015.

[3] Kjellsson E, Hellström G, Perers B. Combination of solar collectors and ground-source heat pump for small buildings. Proceedings of the Solar World Congress, Orlando, Florida, 2005.

[4] Kjellsson E. Solar Colletors Combined with Ground-Source Heat Pumps in Dwellings - Analyses of System Performance. vol. 1018. 2009.

[5] Razavi SH, Ahmadi R, Zahedi A. Modeling, simulation and dynamic control of solar assisted ground source heat pump to provide heating load and DHW. Applied Thermal Engineering 2018;129:127–44. https://doi.org/10.1016/j.applthermaleng.2017.10.003.

[6] Sommerfeldt N, Madani H. Ground Source Heat Pumps for Swedish Multi-Family Houses: Innovative co-generation and thermal storage strategies (Effsys Expand final report) - http://effsysexpand.se/wp-content/uploads/2018/09/EffsysExpandP21-FinalReport_Reviewed.pdf 2018.

[7] Januševičius K, Streckiene G. Solar assisted ground source heat pump performance in nearly zero energy building in Baltic countries. Environmental and Climate Technologies 2013;11:48–56. https://doi.org/10.2478/rtuect-2013-0007.

[8] Miglani S, Orehounig K, Carmeliet J. Integrating a thermal model of ground source heat pumps and solar regeneration within building energy system optimization. Applied Energy 2018;218:78–94. https://doi.org/10.1016/j.apenergy.2018.02.173.

[9] Trillat-Berdal V, Souyri B, Fraisse G. Experimental study of a ground-coupled heat pump combined with thermal solar collectors. Energy and Buildings 2006;38:1477–84. https://doi.org/10.1016/j.enbuild.2006.04.005.

[10] Wang X, Zheng M, Zhang W, Zhang S, Yang T. Experimental study of a solar-assisted ground-coupled heat pump system with solar seasonal thermal storage in severe cold areas. Energy and Buildings 2010;42:2104–10. https://doi.org/10.1016/j.enbuild.2010.06.022.

[11] Verma V, Murugesan K. Experimental study of solar energy storage and space heating using solar assisted ground source heat pump system for Indian climatic conditions. Energy and Buildings 2017;139:569–577. https://doi.org/10.1016/j.enbuild.2017.01.041.

[12] Naranjo-Mendoza C, Oyinlola MA, Wright AJ, Greenough RM. Experimental study of a domestic solar-assisted ground source heat pump with seasonal underground thermal energy storage through shallow boreholes. Applied Thermal Engineering 2019;162:114218. https://doi.org/10.1016/j.applthermaleng.2019.114218.

[13] Huang J, Fan J, Furbo S. Demonstration and optimization of a solar district heating system with ground source heat pumps. Solar Energy 2020;202:171–89. https://doi.org/10.1016/j.solener.2020.03.097.

[14] Sun T, Yang L, Jin L, Luo Z, Zhang Y, Liu Y. A novel solar-assisted ground-source heat pump (SAGSHP) with seasonal heat-storage and heat cascade utilization: Field test and performance analysis. Solar Energy 2020;201:362–72. https://doi.org/10.1016/j.solener.2020.03.030.

[15] Rynkowski P. The Solar-Assisted Vertical Ground Source Heat Pump System in Cold Climates—A Case Study. Proceedings 2020;51:24. https://doi.org/10.3390/proceedings2020051024.

[16] Andersen E, Chen Z, Fan J, Furbo S, Perers B. Investigations of intelligent solar heating systems for single family house. Energy Procedia 2014;48:1–8. https://doi.org/10.1016/j.egypro.2014.02.002.

[17] Haller MY, Yazdanshenas E, Andersen E, Bales C, Streicher W, Furbo S. A method to determine stratification efficiency of thermal energy storage processes independently from storage heat losses. Solar Energy 2010;84:997–1007. https://doi.org/10.1016/j.solener.2010.03.009.

[18] Dragsted J, Furbo S, Dannemand M, Bava F. Thermal stratification built up in hot water tank with different inlet stratifiers. Solar Energy 2017;147:414–25. https://doi.org/10.1016/j.solener.2017.03.008.

[19] Fan J, Chen Z, Furbo S et al. Efficiency and lifetime of solar collectors for solar heating plants. 29th ISES Biennial Solar World Congress. 2009: 331-340.

[20] Summary of EN 12975 Test results, annex to Solar KEYMARK Certification of Kingspan Thermomax solar collectors. "2013. http://www.dincertco.de/.

[21] Furbo S. Hot water tanks for solar heating systems. DTU Byg, Danmarks Tekniske Universitet. Byg Rapport, R-100, 2004.

**Nomenclature**

| | |
|---|---|
| $c$ | fluid specific heat (J/(kg ℃)) |
| $E$ | electricity(kWh) |
| $\dot{E}$ | power (kW) |
| $f$ | fraction |
| $h$ | specific enthalpy (J/kg) |
| $i$ | variable (-) |
| $m$ | mass (kg) |
| $Q$ | energy input/output (kWh) |
| $\dot{Q}$ | heat flow rate (kW) |
| $T$ | temperature (℃) |
| $t$ | operating time ( min) |
| $V$ | volumetric flow rate($m^3/s$) |

*Greek symbols*

| | |
|---|---|
| $\rho$ | fluid density ( $kg/m^3$) |

*Subscripts*

| | |
|---|---|
| a | ambient |
| ac | accumulation |
| bSt | before storage |
| EC | energy change |
| g | ground |
| HP | heat pump |
| in | inlet fluid |
| out | outlet fluid |
| P | pump |
| p | pressure |
| re | renewable |
| SHP | solar and heat pump |
| s | system |
| sol | solar |

Abbreviations

| | |
|---|---|
| BHE | borehole heat exchanger |
| *COP* | coefficient of performance |
| DHW | domestic hot water |
| GHE | ground heat exchanger |

| | |
|---|---|
| HDPE | high density polyethylene |
| HGHE | horizontal ground heat exchanger |
| IPA | isopropyl alcohol |
| PVT | Photovoltaic-Thermal |
| SGHP | solar and ground source heat pump |
| SH | space heating |
| *SPF* | season performance factor |

List of Figures captions